IJIE

The International Journal of Integrated Engineering

Optimization Study on Carbonization of Palm Kernel Shell Using Response Surface Method

O.I Alonge[1], S. O. Obayopo[2]

[1]Department of Mechanical Engineering,
 Elizade University, Ilara-mokin, Ondo State, 340271, NIGERIA

[2]Department of Mechanical Engineering,
 Obafemi Awolowo University, Ile-Ife, 220282, NIGERIA

*Corresponding author.

Abstract: The carbonization of Palm Kernel Shell (PKS) was carried out in a constant volume reactor and the optimization of the important factors (Temperature, Particle Size, and Residence time) that affect the quality of the biochar product was investigated using Response Surface Method (RSM-CCD). The characterization results before carbonization show that PKS is a potential biomass to be considered as an alternative for fossil fuel. Center Composite Design (CCD) was employed in the carbonization process to investigate the effect of process parameters on the quality of biochar formed. The optimized conditions obtained for fixed carbon yield were temperature of 469.16ºC, the particle size of $0.8 < x \leq 1$mm, the residence time of 17.68 min, and these optimized conditions gave a fixed carbon of 79.65 % with a corresponding yield of 34.00 %, while the temperature was observed to be the most influential factor. The optimized conditions were validated, and the predicted results were in good agreement with the experimental results, as the relative error between the predicted and experimental values for the fixed carbon and corresponding percentage yield were -1.26 and 0.36 %, respectively. The study revealed the potential of PKS at different particle sizes considered, to be used as solid fuel.

Keywords: Carbonization, PKS, constant volume reactor, temperature, particle size, residence time

1. Introduction

The rapid depletion of natural reserves, as well as the expensive methods used in their extraction, has resulted in a rapid decline in the quantity of fossil fuel yield all over the world [1]. Fossil fuels are non-renewable, their primary supplies will be consumed eventually, and their use is frequently connected with significant environmental impact. Alternatively, renewable and clean energy sources have been tapped and invested in by governments. Biomass and some other green energy sources have rekindled interest and are once again making headlines as viable solutions to fossil fuels' shortcomings [2]. Biomass is a carbon-free, abundant, and inexpensive fuel, but it has a poor energy density. Its energy can either be released directly as heat through combustion or captured by turning biomass into more energy-dense biofuels. One such biomass resources is palm kernel shell. Nigeria has the largest palm oil groves worldwide, estimated at 2.1 -2.3 million hectares. These groves supplied the world market with palm oil and palm kernels before the crop became cultivated in other parts of the world [3]. However, the oil deriving rate is only 10% from palm oil production with the majority of 90% left as waste. These wastes, in the form of biomass, include empty fruit bunch, palm kernel shell, and mesocarp fiber, and about 0.007 tons of palm shell, 0.103 tons of palm fiber, and 0.012 tons of kernel are produced as solid waste for every ton of oil-palm fruit bunch [4]. Out of these oil palm wastes,

palm kernel shell (PKS) has been reported to have the highest energy content, the highest amount of lignin, and low hemicellulose which is favorable for char synthesis [5].

When processed properly, biomass can also be used to replace coal in the primary energy mix. Torrefaction, liquefaction, pyrolysis, and gasification methods have all aimed to extract energy from biomass and convert it into solid, liquid, or gaseous biofuels [6]. Pyrolysis is one of the most promising methods for converting biomass to fuel. Because no wastage is generated during the process, this technology has been acknowledged as an eco-friendly alternative [7]. Traditional or slow pyrolysis, also known as carbonization techniques, is used to optimize solid biochar products by operating with slow heating rates and lengthy residence durations. Other carbonization techniques, such as Flash carbonization, hydrothermal carbonization (HTC), and constant-volume carbonization (CVC), have recently been developed to increase the yield and/or quality of solid products [6]. The final biochar product made through carbonization processes can be used for several things, including fuel for cooking and barbecuing, heat and power generation, an adsorbent for removing pollutants from air or water streams, the development of advanced carbon materials, super-capacitors, hydrogen storage, and as a natural soil amendment to sequester carbon and improve soil quality [8].

Constant volume carbonization is the process of carbonization whereby the reactor is covered to ensure a constant volume of the substance in the reactor. CVC provides more control over the carbonization process than other carbonization methods including conventional carbonization and hydrothermal carbonization, and the resulting biochar has higher fixed-carbon yields [6]. Some recent works have reported the proximate analysis of the char derived from the thermal conversion of cellulose in open and closed reactors. When the reactor is entirely sealed, fixed carbon derived is close to the equilibrium limiting value, but when the reactor is left exposed to the environment, fixed carbon yields are well below the theoretical maximum anticipated at equilibrium. The longer residence durations and greater partial pressure of the volatile vapor inside and around the carbonaceous particles help to explain the improvement in the characteristics of the char formed at high pressures. These two variables have been found to be essential for enhancing the subsequent, heterogeneous charring reaction between hot char and tarry vapor [9]. A review of the effect of process parameters on the production of biochar from biomass waste through pyrolysis has been carried out and out of the parameters highlighted, the most important parameters that affect product yield are temperature, residence time, and particle size [10]. This study, therefore, aims at optimizing the utilization of PKS through constant volume carbonization to produce biochar of high quality.

2. Materials and Methodology

2.1 Materials Preparation and Characterization

The raw palm kernel shell was collected at the local oil palm processing industry at Ilara-mokin, Ondo State, and was sun-dried for three days for characterization until the moisture content was within 10-16% appropriate moisture level for solid fuel, as recommended by ASTMD2016-25 [11]. The palm kernel shell was ground using a grinding machine and sieved into three particle sizes (<0.6, $0.6 \leq x \leq 0.8$, $0.8 < x \leq 1$ mm) using an SV0005 electromagnetic sieve shaker at Elizade University, Nigeria and they are as shown in Fig. 1. Proximate analysis of the samples was carried out using various methods as shown in Table 1.

Table 1 - Methods employed for proximate analysis

Property	Analytical Method (Standard)
Moisture Content (MC)	ASTM D871
Volatile Matter (VM)	ASTM E872
Ash Content (AC)	ASTM D1102
Fixed Carbon (FC = 100-VM-AC-MC)	By difference
Ultimate Analysis	BSI, 1974

Fig. 1 - Palm Kernel in Different Particle Sizes (a) < 0.6 mm; (b) $0.6 \leq x \leq 0.8$ mm; (c) $0.8 < x \leq 1$ mm

2.2 Experimental Design for the Carbonization Modelling

Response Surface Method was used to determine the optimal parameters for the carbonization process. It was used to find the optimal process settings and troubleshoot process problems and weak points. In this study, the major factors (temperature, residence time, and particle size) that contribute to the devolatilization of biomass as reported in the literature were considered. Slow pyrolysis involves heating biomass up to temperatures between 400 and 500 °C at a rate of around 0.1 and 1 °C/s over a period between 5 and 30 min [10]. Three levels of temperature (400°C, 450°C, and 500°C) and residence time (15, 20, and 25 minutes) together with the particle sizes (<0.6, $0.6 \leq x \leq 0.8$, $0.8 < x \leq 1$ mm), were considered for this study. The experimental design matrix that was employed in this study is the Composite Centered Design (CCD) model which is a second-order model (Equ. 1) that includes factorial points, axial points, and augmented central points. The model checks the significant effect of each of the parameters, as well as the optimization of the response as the function of the independent variables. In this study, Design-Expert Software Version 8.0.0 (Stat-Ease, Inc., Minneapolis, USA) was used to design the experiments. The number of runs generated is shown in Table 2 and Table 3. The model competencies were checked with the values of R^2 and adjusted R^2. The authentication of the optimized conditions was done in duplicate to establish the strength of the model.

$$Y = \beta_0 + \sum_{i=1}^{K} \beta_i x_i + \sum_{i=1}^{K} \beta_{ii} x_i^2 + \sum_{i=1}^{K} \beta_{ij} x_i x_j + \varepsilon \qquad (1)$$

Where β_0 is the intercept, β_i is the linear coefficient, β_{ii} is the squared coefficient, β_{ij} is the interaction coefficient, $x_i \ and \ x_j$ are the factors.

2.3 Carbonization Process

The carbonization process was carried out using a fixed bed reactor shown in Fig. 2. The reactor is cylindrical of a batch type with a useful volume of 636.3 cm³. Heating was provided by a cylindrical ceramics band heating element with a power of 1.5 kW making it possible to work at temperatures up to 800°C. The reaction temperature was monitored by a type K thermocouple inserted through the side of the lagged body and positioned at a side corner of the heating element. For each experimental run designed, 30g of sample was loaded. A gasket was placed on the reactor before the cover was completely bolted to ensure a hermetically sealed reactor, in other to prevent any trace of volume loss and to ensure a constant volume process. After the carbonization process, proximate analysis was carried out on the carbonized samples. It was observed that a coke-like solid was formed on the wall of the reactor after the carbonization process as shown in Figure 3.
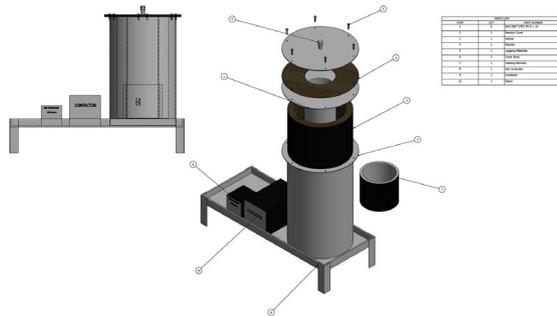

Fig. 2 - A constant volume fixed bed reactor

Fig. 3 - Coke formed on the wall of the reactor

3. Result and Discussion

3.1 Proximate and Ultimate Analysis

The results of the proximate and ultimate analysis are shown in Table 4. Due to endothermic evaporation, moisture content influences both the internal temperature history of the solid and the amount of energy required to raise the solid to the pyrolytic temperature [13]. The particle sizes taken into consideration are all low moisture fuels (6% to 16%), making them viable as fuel for energy production. Particle sizes below 10% are often regarded as appropriate for thermochemical conversion. Particle size <0.6 had ash content greater than 4% as recommended for agricultural residue and less than 8% recommended for superior coal while samples $0.6 \leq x \leq 0.8$ and $0.8 < x \leq 1$ mm have ash content less than 4%. The particle size <0.6 also had the lowest amount of fixed carbon and this implies that it will be less reactive compared with particle sizes $0.6 \leq x \leq 0.8$ mm and $0.8 < x \leq 1$ mm. The higher the fixed carbon content of a fuel, the more reactive the fuel [14]. When the particle size is increased, the vapour formed during the thermal cracking of biomass covers more distance via the char layer, which results in more secondary reactions leading to the

generation of char [10]. The ultimate analysis showed that the samples considered contain a higher amount of carbon content, which indicates that those particle sizes are viable for energy production, and the higher the carbon content, the higher the calorific value and the better the quality of the biomass for power generation. The higher the particle size, the higher the amount of carbon. The low amount of nitrogen and Sulphur indicates that during carbonization, the formation of SOx and NOx will be less.

Table 2 - Specification of variables and the experimental domain

Independent Variable	Code	Experimental Domain		
		-1	0	+1
A: Temperature (ºC)	X_1	400	450	500
B: Particle Size	X_2	< 0.6	$0.6 \leq x \leq 0.8$	$0.8 < x \leq 1$
C: Reaction Time (min)	X_3	15	20	25

Table 3 - CCD design matrix

Run	Factor 1 A: Temperature ºC	Factor 2 B: Residence Time K	Factor 3 C: Particle Size Min
1	500	25	$0.8 < x \leq 1$
2	500	15	$0.8 < x \leq 1$
3	450	20	< 0.6
4	450	20	$0.6 \leq x \leq 0.8$
5	500	25	< 0.6
6	400	20	$0.6 \leq x \leq 0.8$
7	400	15	$0.8 < x \leq 1$
8	400	25	$0.8 < x \leq 1$
9	500	20	$0.6 \leq x \leq 0.8$
10	450	20	$0.8 < x \leq 1$
11	400	15	<0.6
12	400	25	<0.6
13	450	15	$0.6 \leq x \leq 0.8$
14	450	20	$0.6 \leq x \leq 0.8$
15	450	20	$0.6 \leq x \leq 0.8$
16	450	25	$0.6 \leq x \leq 0.8$
17	500	15	<0.6

3.2 Statistical Data Analysis of the Optimization Process

The result of the carbonization process for fixed carbon and percentage yield response using the CCD experimental design is presented in Tables 5 and 6, respectively. The results also showed the predicted values, percentage standard deviation, and residuals. Small residual values and standard deviation obtained show that the degree of deviance of the experimental value from the predicted values is very minimal. The quadratic regression model that best describes the fixed carbon is given by Equ. 2, while the linear regression model that describes percentage yield is given by Eq. 3.

$$Y_{Fixed\ Carbon} = 79.21 + 4.19A - 0.060B + 6.25C + 1.12AB - 1.71AC - 2.39BC - 2.57A^2 - 2.20\ B^2 + 1.11C^2$$

(2)

$$Y_{\%\ Yield} = 35.21 - 3.57A - 0.6930B - 0.1610C$$

(3)

Table 4 - Proximate analysis of raw samples

Analysis/Particle Sizes	< 0.6 mm	$0.6 \leq x \leq 0.8$mm	$0.8 < x \leq 1$mm
Moisture Content (%)	8.31	8.73	8.47
Fixed Carbon (%)	16.06	23.02	24.76
Volatile Matter (%)	67.52	66.47	65.63
Ash Content (%)	8.11	1.78	1.14
Carbon (%)	41.25	45.21	45.92
Hydrogen (%)	5.08	5.36	5.41
Oxygen (%)	44.15	46.17	46.21
Sulphur (%)	0.17	0.28	0.19
Nitrogen (%)	1.24	1.19	1.13
Energy Content (MJ/kg)	15.94	17.27	17.53

Table 5 - CCD values for fixed carbon surface response analysis

S/N	A (ºC)	B (min)	C (mm)	Observed Fixed Carbon (%)	Predicted Fixed Carbon (%)	%SD	Residual	Volatile Matter (%)	Ash Content (%)
1	500	25	$0.8 < x \leq 1$	73.83	75.00	0.83	-1.17	23.91	2.26
2	500	15	$0.8 < x \leq 1$	78.10	77.67	0.30	0.4314	18.14	3.72
3	450	20	<0.6	66.11	66.12	0.01	-0.0105	25.14	8.76
4	450	20	$0.6 \leq x \leq 0.8$	70.95	71.27	0.23	-0.3173	26.17	2.89
5	500	25	<0.6	71.13	70.70	0.30	0.4294	19.90	8.98
6	400	20	$0.6 \leq x \leq 0.8$	64.69	64.50	0.13	0.1875	33.04	2.27
7	400	15	$0.8 < x \leq 1$	74.24	74.94	0.49	-0.7046	24.13	1.63
8	400	25	$0.8 < x \leq 1$	68.13	67.80	0.23	0.3304	30.07	1.80
9	500	20	$0.6 \leq x \leq 0.8$	73.80	72.89	0.64	0.9135	23.38	2.82
10	450	20	$0.8 < x \leq 1$	79.74	78.63	0.78	1.11	17.23	3.05
11	400	15	<0.6	55.12	54.23	0.63	0.8934	37.09	7.79
12	400	25	<0.6	55.95	56.66	0.50	-0.7066	36.29	7.76
13	450	15	$0.6 \leq x \leq 0.8$	69.11	69.12	0.01	-0.0145	26.32	4.57
14	450	20	$0.6 \leq x \leq 0.8$	70.15	71.27	0.79	-1.12	26.97	2.89
15	450	20	$0.6 \leq x \leq 0.8$	70.50	71.27	0.54	-0.7673	26.77	2.87
16	450	25	$0.6 \leq x \leq 0.8$	70.12	69.00	0.79	1.12	25.89	3.99
17	500	15	<0.6	63.19	63.80	0.43	-0.6056	27.54	9.28

Table 6 - CCD values for percentage yield surface response analysis

S/N	A (ºC)	B (min)	C (mm)	Actual Percentage Yield (%)	Predicted Percentage Yield (%)	%SD	Residual
1	500	25	$0.8 < x \leq 1$	30.90	30.79	0.08	0.1116
2	500	15	$0.8 < x \leq 1$	32.13	32.17	0.03	-0.0444
3	450	20	<0.6	34.75	35.37	0.44	-0.6234
4	450	20	$0.6 \leq x \leq 0.8$	35.42	35.21	0.15	0.2076
5	500	25	<0.6	31.38	31.11	0.19	0.2696
6	400	20	$0.6 \leq x \leq 0.8$	38.44	38.78	0.24	-0.3424
7	400	15	$0.8 < x \leq 1$	39.60	39.31	0.21	0.2856
8	400	25	$0.8 < x \leq 1$	37.62	37.93	0.22	-0.3084
9	500	20	$0.6 \leq x \leq 0.8$	31.30	31.64	0.24	-0.3424
10	450	20	$0.8 < x \leq 1$	35.02	35.05	0.02	-0.0314
11	400	15	<0.6	40.05	39.64	0.29	0.4136
12	400	25	<0.6	38.20	38.25	0.04	-0.0504
13	450	15	$0.6 \leq x \leq 0.8$	35.61	35.91	0.21	-0.2954
14	450	20	$0.6 \leq x \leq 0.8$	35.54	35.21	0.23	-0.3276
15	450	20	$0.6 \leq x \leq 0.8$	35.29	35.21	0.06	0.0776
16	450	25	$0.6 \leq x \leq 0.8$	34.86	34.52	0.24	0.3406
17	500	15	<0.6	32.50	32.50	0.04	0.0036

The Sequential model sum of the square test was performed to check the adequacy of the model generated from the obtained data and results are given in Table 7 for fixed carbon and in Table 8 for percentage yield. The quadratic versus

two-factor interaction (2FI) model has a p-value <0.05 for fixed carbon and it was suggested while the linear versus mean model has a P-value <0.05 for percentage yield and was suggested for the analysis of the results. The summary of the analysis of variance (ANOVA) for the selected quadratic model for fixed carbon is shown in Table 9 while the ANOVA for the linear model for percentage yield is shown in Table 10. The ANOVA demonstrated that the model is significant from the P-value obtained which is less than 0.05. For fixed carbon, all the terms (A, C, AC, BC, A^2, and B^2) are significant (P<0.05) with their respective P value less than 0.05 while B and C^2 are not significant (P>0.05). In the case of percentage yield response, only the terms A and B are significant (P <0.05) while the model term C is not significant (P >0.05). The lack of fit obtained was not significant for both models. Therefore, the models adequately explain the variation in the responses. Also, the predicted and adjusted R^2 are reasonably high values and in reasonable agreement as the difference is less than 0.2 which implies that the experimental data can be explained by the model. The values of adjusted R^2 for fixed carbon and percentage yield are 0.9701 and 0.9869, respectively. Also, comparison plots of the predicted values against the actual values for fixed carbon and percentage yield are shown in Fig. 4 and these plots support the high value of R^2. These results imply that the model derived from RSM-CCD can be used adequately to describe the relationship between the input variables and the responses.

Table 7 - Model summary statistics for Palm Kernel using fixed carbon response

Source	Sum of Squares	df	Mean Square	F-value	p-value	
Mean vs Total	81173.15	1	81173.15			
Linear vs Mean	566.89	3	188.96	17.29	< 0.0001	
2FI vs Linear	79.28	3	26.43	4.21	0.0362	
Quadratic vs 2FI	**53.25**	**3**	**17.75**	**13.02**	**0.0030**	**Suggested**
Cubic vs Quadratic	5.39	4	1.35	0.9719	0.5308	Aliased
Residual	4.16	3	1.39			
Total	81882.11	17	4816.59			

Table 8 - Model summary statistics for Palm Kernel using percentage yield response

Source	Sum of Squares	df	Mean Square	F-value	p-value	
Mean vs Total	21073.54	1	21073.54			
Linear vs Mean	**132.51**	**3**	**44.17**	**416.41**	**< 0.0001**	**Suggested**
2FI vs Linear	0.2850	3	0.0950	0.8686	0.4891	
Quadratic vs 2FI	0.2010	3	0.0670	0.5254	0.6786	
Cubic vs Quadratic	0.4719	4	0.1180	0.8408	0.5804	Aliased
Residual	0.4210	3	0.1403			
Total	21207.43	17	1247.50			

Table 9 - ANOVA for response surface quadratic model for Palm Kernel using fixed carbon response

Source	Sum of Squares	df	Mean Square	F-value	p-value	
Model	699.42	9	77.71	57.01	< 0.0001	significant
A-Temperature	175.73	1	175.73	128.91	< 0.0001	
B-Residence Time	0.0360	1	0.0360	0.0264	0.8755	
C-Particle Size	391.13	1	391.13	286.92	< 0.0001	
AB	10.01	1	10.01	7.35	0.0302	
AC	23.43	1	23.43	17.19	0.0043	
BC	45.84	1	45.84	33.63	0.0007	
A²	17.59	1	17.59	12.90	0.0088	
B²	12.88	1	12.88	9.45	0.0180	
C²	3.35	1	3.35	2.46	0.1611	
Residual	9.54	7	1.36			
Lack of Fit	9.20	5	1.84	10.61	0.0884	not significant
Pure Error	0.3467	2	0.1733			
Cor Total	708.96	16				
Adjusted R^2 = 0.9701			Predicted R^2 = 0.8418			

Table 10 - ANOVA for response surface quadratic model for Palm Kernel using percentage yield response

Source	Sum of Squares	df	Mean Square	F-value	p-value	
Model	132.51	3	44.17	404.03	< 0.0001	significant
A-Temperature	127.45	1	127.45	1165.80	< 0.0001	
B-Residence Time	4.80	1	4.80	43.93	< 0.0001	
C-Particle Size	0.2592	1	0.2592	2.37	0.1476	
Residual	1.42	13	0.1093			
Lack of Fit	1.39	11	0.1264	8.08	0.1152	not significant
Pure Error	0.0313	2	0.0156			
Cor Total	133.93	16				
Adjusted R^2 = 0.9869			Predicted R^2 = 0.9820			
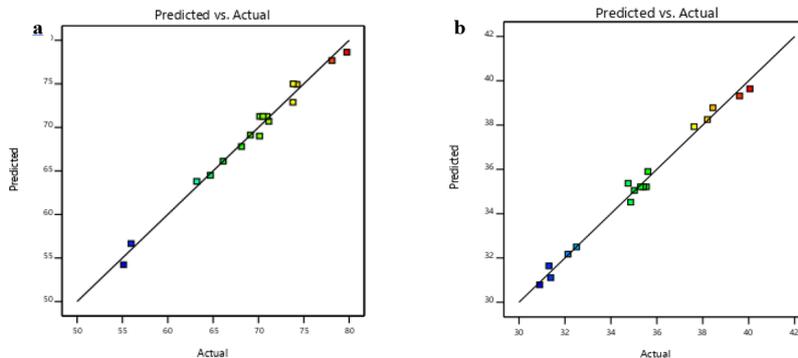
Fig. 4 - Plots of predicted values against the actual values (a) fixed carbon; (b) percentage yield

3.3 Interactive Effect of Factors on Fixed Carbon

The interactive effect of the three factors considered was examined by plotting 3-D graphs as shown in Fig. 5. The curvature nature of the graphs shows that there are significant interactions among the factors considered. The maximum fixed carbon obtained was 79.74% at a temperature of 450 °C, residence time of 20 min, and at a particle size of $0.8 < x \leq 1$ mm while the lowest obtained was 55.12 % at a temperature of 400 °C, residence time of 15 min, and at particle size <0.6 mm. In Fig. 5a, the contour shows that as the temperature increases the number of fixed carbon increases while the effect of residence time was insignificant. Therefore, the temperature is the more significant factor as the two factors interact. In Fig. 5b, as the particle size increases with an increase in temperature, there was an increase in fixed carbon yield, and the maximum yield was obtained at particle size $0.8 < x \leq 1$ mm at a temperature above 450 °C. In Fig. 5c, as the particle size increases, the effect of residence time becomes noticeable as high fixed carbon was observed at a residence time of 20 min and below at a particle size of $0.8 < x \leq 1$ mm. This result showed that it is possible to achieve high fixed carbon at a lower residence time. It was also observed that at high residence time, burning out of the carbonaceous residue began and this could be the reason for the reduction in fixed carbon at high residence time. It becomes imperative that the optimal residence time should be determined. Carbonizing high particle size biomass at low residence time will result in char that is low in fixed carbon. Therefore, to produce char that is rich in fixed carbon, the higher the particle size, the longer the biomass should stay in the reactor. The increase in fixed carbon as the residence time increased was the result of repolymerization of the biomass constituents which gave them enough time to react, while at the lesser time, repolymerization of biomass constituents did not get completed and the fixed carbon was reduced [10]. Also, an increase in the temperature allows the thermal cracking of heavy hydrocarbons leading to a char with high fixed carbon.

3.4 Interactive Effect of Factors on Percentage Yield

There was no interactive effect, as the model is linear, while only individual factor effect on percentage yield was observed, and it was examined by plotting 2-D line graphs as shown in Fig. 6. The maximum yield obtained was 40.05% at a temperature of 400 °C, the residence time of 20 min, and a particle size of <0.6 mm while the lowest obtained was 30.9% at a temperature of 500 °C, the residence time of 25 min and particle size of $0.8 < x \leq 1$ mm. In Fig. 6a, the line graph shows that as the temperature increases the percentage yield decreases. The effect of thermal cracking was significant as it reduces the percentage yield as the temperature increases. In Fig. 6b, it was observed that the percentage yield decreases as the residence time increases. The longer the residence time, the more the thermal cracking and the lesser the char yield [10], while in Fig. 6c, the effect of particle size is insignificant to the change in percentage yield.
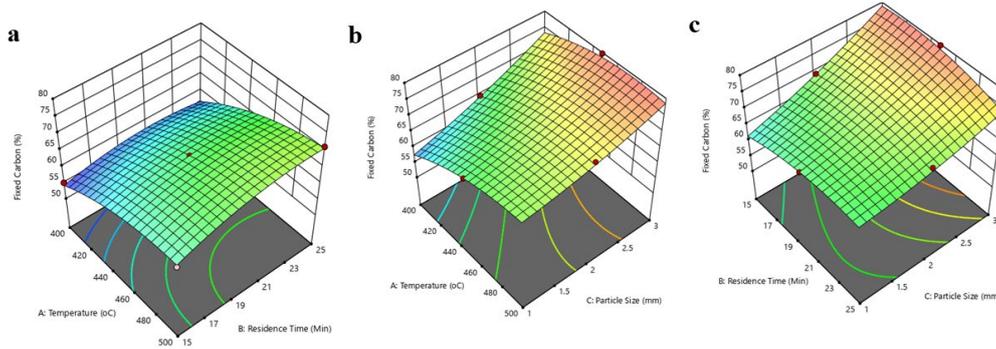
Fig. 5 - Contour and surface plots of the interactive effect of factors on fixed carbon (a) temperature vs residence time; (b) temperature vs particle size; (c) residence time vs particle size
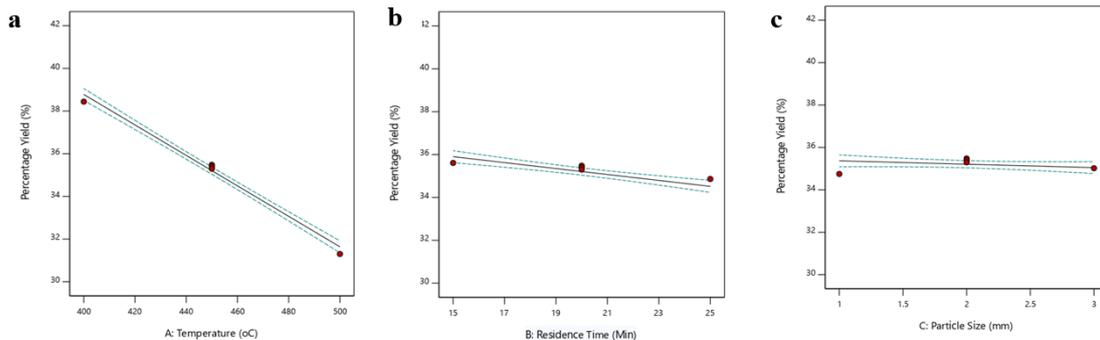

Fig. 6 - Linear plots of the interactive effect of factors on percentage yield (a) percentage yield vs temperature; (b) percentage yield vs residence time; (c) percentage yield vs particle size

3.5 Verification of Optimized Condition and Predictive Model

A numerical optimization approach was used to establish the best experimental condition to get the optimal fixed carbon with the corresponding percentage yield. To find a good set of conditions that will meet all goals, the three variables were set in range while the responses were set as "maximum". By applying the desirability function approach, the optimum values were numerically predicted as a temperature of 469.16°C, a residence time of 17.68 min, and a particle size of $0.8 < x \leq 1$ mm. The predicted fixed carbon yield under the optimum values was 79.65% and the corresponding predicted percentage yield was 34.00%. An experiment was carried out to validate the optimized conditions. As shown in Table 11, the experimental data were in good agreement with the predicted values, as the relative error between the predicted and experimental values for the fixed carbon and percentage yield were -1.26 and 0.36 %, respectively.

Table 11 - Experimental validation of predicted values at optimal conditions

Sample	Predicted F.C (%)	Expr. F.C (%)	Relative Error[a] (F.C) (%)	Predicted Yield (%)	Expr. Yield (%)	Relative Error[a] (Yield) (%)
Palm Kernel $X_1 = 469.16$ oC $X_2 = 0.8 < x \leq 1$mm $X_3 = 17.68$ min	79.65	78.66	-1.26	34.00	36.25	0.36

[a]Relative error (%) = [(experimental value − predicted value)/experimental value] × 100%.

4. Conclusion

The design and operating conditions of the fixed bed were suitable for the carbonization process under constant volume. The Response Surface Method/Center Composite Design was very successful in determining the correlation between the experimental factors (temperature, particle size, and residence time) and the responses (fixed carbon and percentage Yield). The regression model for predicting the amount of fixed carbon and the corresponding percentage yield was also developed. The values of adjusted R^2 for fixed carbon and percentage yield were 0.9701 and 0.9869, respectively. Based on these values the model obtained was demonstrated to be efficient both in prediction capability

and data fitting. The models established the optimum values for the carbonization process at a temperature of 469.16 ºC, a particle size of $0.8 < x \leq 1$ mm, and a residence time of 17.68 min, which gives a fixed carbon yield of 79.65% with a corresponding percentage yield of 34.00%. In this study, among the three parameters considered, the temperature was found to be the most significant that affects the fixed carbon of palm kernel and the corresponding percentage yield. Future studies may look at the effect of more factors on the carbonization of palm kernel shell and carry out performance evaluation of the biochar produced from the optimal parameters.

Acknowledgment

References

[1] Wu, X., Markham, J., Sun, X. S., & Wang, D. (2012). Optimizing catalytic fast pyrolysis of biomass for hydrocarbon yield. American Society of Agricultural and Biological Engineers, 55(5), 1879‑1885.

[2] Rodrigue, J. P., Comtois, C., & Slack, B. (2016). The Geography of Transport Systems; Taylor & Francis.

[3] Gold, I. L., Ikuenobe, C. E., Asemota, O., & Okiy, D. A. (2012). Palm and palm kernel oil production and processing in Nigeria. Nigerian Institute for Oil Palm Research (NIFOR), Benin City, Edo State, Nigeria.

[4] Pansamut, V., Pongrit, V., & Intarangsi, C. (2003). The oil palm. Department of Alternative Energy Development and Efficiency. Ministry of Energy, Thailand.

[5] Xin, J. L., Lai, Y. L., Suyin, G., Suchithra, T., & Hoon K. N. (2017). Biochar potential evaluation of palm oil wastes through slow pyrolysis: Thermochemical characterization and pyrolytic kinetic studies. Bioresource Technology, 236, 155–163.

[6] Maider, L., Trevor, M., Scott, T., Liang W., Øyvind S., & Michael J. (2019). Effect of Processing Conditions on the Constant-Volume Carbonization of Biomass. Energy Fuels, 33, 2219−2235.

[7] Bridgwater, T. (2006). Biomass for energy. Journal of the Science of Food and Agriculture, 86(12), 1755-1768.

[8] Chiaramonti, D., Prussi, M., Nistri, R., Pettorali, M., & Rizzo, A. M. (2014). Biomass Carbonization: Process Options and Economics for Small Scale Forestry Farms. Energy Procedia, 61, 1515–1518.

[9] Wesenbeeck, S. V., Higashi, C., Legarra, M., Wang, L., & Michael Jerry Antal, J. (2016). Biomass Pyrolysis in Sealed Vessels. Fixed-Carbon Yields from Avicel Cellulose That Realize the Theoretical Limit. Energy & Fuels, 30 (1), 480–491.

[10] Tripathi, M., Sahu, J.N., & Ganesan, P. (2016). Effect of process parameters on production of biochar from biomass waste through pyrolysis: A review. Renewable and Sustainable Energy Reviews 55: 467–481.

[11] Debdoubi, A., Cano, J., Kiveka, R., & E. (2004). Colacio, Production of fuel briquettes from esparto partially pyrolyzed. Energy Conversion and Management, 46, 1877–1884.

[12] Friedl, A., Padouvas, E., Rotter, H., & Varmuza, K. (2005) Prediction of heating values of biomass fuel from elemental composition. Anal. Chim. Acta, 544 (1−2), 191−198.

[13] Elehinafe, F. B., Okedere, O. B., Fakinle, B. and Sonibare, J. A. (2019). Assessment of sawdust of different wood species in Southwestern Nigeria as source of energy. *Energy Sources Part A: Recovery, Utilization and Environmental Effects*, 10, 84-89.

[14] Abdu-Zubairu, S. A. (2014). Production and characterization of briquette charcoal by carbonization of agro-waste. *Journal of Energy and Power*, 4(2), 41-47.